NASA TECHNICAL NOTE

NASA TN D-2838

EXPERIMENTAL PRESSURE-DROP INVESTIGATION OF NONWETTING, CONDENSING FLOW OF MERCURY VAPOR IN A CONSTANT-DIAMETER TUBE IN 1-G AND ZERO-GRAVITY ENVIRONMENTS

by James A. Albers and Robert P. Macosko

Lewis Research Center
Cleveland, Ohio

NATIONAL AERONAUTICS AND SPACE ADMINISTRATION • WASHINGTON, D. C. • JUNE 1965

C.1
Completed
19 oct 66
mrt

ERRATA

NASA Technical Note D-2838

EXPERIMENTAL PRESSURE-DROP INVESTIGATION OF NONWETTING, CONDENSING FLOW OF MERCURY VAPOR IN A CONSTANT-DIAMETER TUBE IN 1-g AND ZERO-GRAVITY ENVIRONMENTS

by James A. Albers and Robert P. Macosko

June 1965

Page 2: The following information should be added at the end of the INTRODUCTION:

A 16 mm film (color and sound) which describes the testing and hardware used in the MECA zero-gravity program is available through the Lewis Research Center. The motion picture (C-221), entitled Two-Phase Mercury Flow in Zero Gravity, also presents high-speed films of mercury condensing in constant-diameter glass tubes.

Film C-221 is available on request to

Chief, Technical Information Division
National Aeronautics and Space Administration
Lewis Research Center
21000 Brookpark Road
Cleveland, Ohio 44135

Page 5, paragraph 2: Line 5 should read

by pressurizing the gas side of the bladder with regulated gaseous nitrogen.

Page 7: Figure 1(d) should be replaced by the corrected figure attached.

Page 14: Figure 5 should be replaced by the corrected figure attached.

NASA-Langley, 1966

Issued 9-19-66

NASA TN D-2838

EXPERIMENTAL PRESSURE-DROP INVESTIGATION OF NONWETTING, CONDENSING FLOW OF MERCURY VAPOR IN A CONSTANT-DIAMETER TUBE IN 1-G AND ZERO-GRAVITY ENVIRONMENTS

By James A. Albers and Robert P. Macosko

Lewis Research Center
Cleveland, Ohio

NATIONAL AERONAUTICS AND SPACE ADMINISTRATION

For sale by the Clearinghouse for Federal Scientific and Technical Information
Springfield, Virginia 22151 – Price $2.00

EXPERIMENTAL PRESSURE-DROP INVESTIGATION OF NONWETTING, CONDENSING FLOW OF MERCURY VAPOR IN A CONSTANT-DIAMETER TUBE IN 1-G AND ZERO-GRAVITY ENVIRONMENTS

by James A. Albers and Robert P. Macosko

Lewis Research Center

SUMMARY

An experimental investigation was conducted to determine the differences between the pressure losses of nonwetting (dropwise) condensing flow of mercury vapor in 1-g and zero-gravity environments. Local and overall pressure-drop data were obtained for a horizontal, constant-diameter, stainless-steel tube for various flow rates, pressures, and condensing lengths.

The measured overall static pressure drop indicated little difference between 1-g and zero-gravity pressure losses at flow rates of approximately 0.028 and 0.046 pound mass per second. The overall static pressure drop varied from 0.20 to 2.24 pounds per square inch, while the total pressure loss varied from 1.4 to 5.4 pounds per square inch for the condensing lengths and the flow rates considered.

The Lockhart-Martinelli correlation predicts Φ_g, within ±30 percent and, $(\Delta P/\Delta L)_{TP}$, within ±70 percent for the high velocity, high quality region of the condensing tube. The pressure gradients both for 1 g and zero gravity are greater than predicted by Lockhart-Martinelli for the low quality region of the tube. Generally, the data trend correlates with the fog-flow theory. The data indicate that the fog-flow parameter approaches 1 for high values of the Weber number. The data spread is least in the high-velocity (high-Weber-number) region of the tube that approaches the fog-flow regime. For the preceding local plots, the effect of gravity was negligible.

INTRODUCTION

There have been many energy-conversion-system concepts proposed for the generation of electric power for various space-flight missions. One of the

more promising of these for the production of high power levels is the liquid metal Rankine cycle turbogenerator system utilizing either nuclear or solar energy as the primary heat source. The interest in this type of power system is characterized by the development of the SNAP-1, SNAP-2, Sunflower, and currently the SNAP-8 and SNAP-50 systems. A characteristic of the Rankine cycle systems is that the working fluid in the turbogenerator loop undergoes phase changes during the heat-addition and heat-rejection portions of the cycle. The liquid and vapor coexist in continuously varying proportions between the all-liquid and saturated vapor states. These variable quality flow conditions represent a major problem in the design of the boiler and condenser components with regard to the prediction of heat transfer, pressure drop, and dynamic stability characteristics. Furthermore, the mixed-phase flows are subject to effects of differing gravity fields to the extent that data on heat transfer, pressure drop, and dynamic stability obtained in a 1-g environment may not be representative of those to be encountered during system operation in a weightless condition. One of the particularly critical flow problems associated with the condensing process is that of pressure drop. Condensation occurs in the low-pressure portion of the cycle and is restricted to a rather stringent pressure-drop budget imposed, on one end, by the turbine exit pressure, and on the other by the net positive suction head requirement of the recirculating pump. Because of these considerations, an experimental program was initiated at the NASA Lewis Research Center to determine the condensing two-phase pressure-drop characteristics under 1-g and zero-gravity environments.

Previous analytical studies of the two-phase flow problem have dealt with simplified flow models to derive correlations that would permit the estimation of two-phase pressure drops (from single-phase pressure-drop measurement). Experimental data have been acquired for two-component two-phase adiabatic flows by Lockhart and Martinelli (ref. 1). A modification of the Lockhart-Martinelli flow model is discussed in reference 2. Experimental and analytical studies of mercury condensing are discussed in references 3 to 7.

The primary purpose of this investigation was to determine the effect of weightlessness on the condensing two-phase flow process with particular emphasis on the local and overall pressure drops for condensing mercury. The secondary purpose of this investigation was to compare the measured local pressure gradients with the analytical predictions of Lockhart-Martinelli and of Koestel, et al. (refs. 1 and 7, respectively).

The aircraft zero-gravity maneuver and the vertical accelerations obtained in this investigation are discussed in appendix A by Clifford C. Crabs.

added – see insets attached to front cover

SYMBOLS

A area, sq ft

c_p specific heat, Btu/(lb mass)($^\circ$F)

D tube inside diameter, ft

D_m diameter of flow passage formed by drops on wall through which fog flows, ft

E_σ	experimental constant, dimensionless
f	friction factor, dimensionless
f	function of
G	mass velocity, lb/(sec)(sq ft)
g_c	conversion factor, 32.174 (lb mass)(ft)/(lb force)(sec^2)
h	convective heat-transfer coefficient, Btu/(sec)(sq ft)(^oF)
h_{fg}	latent heat of vaporization, Btu/(lb mass)
k	conductivity, Btu/(sec)(ft)(^oF)
L	length, ft
l	distance from condensing tube inlet, ft
l_c	condensing length, ft
P	pressure, lb/sq ft
q	heat flux, Btu/(hr)(sq ft)
R	thermal resistance, (sec)(sq ft)(^oF)/Btu
Re	Reynolds number, dimensionless
t	thickness, ft
U	overall heat-transfer coefficient, Btu/(sec)(sq ft)(^oF)
u	velocity, ft/sec
v	specific volume, (cu ft)/(lb mass)
w	mass flow rate, (lb mass)/sec
x	quality, w_g/w_T, dimensionless
Δ	finite differential
ϵ	slip ratio, $(u_g - u_{liq})/u_g$, dimensionless
μ	viscosity, lb mass/(ft)(sec)
ρ	density, lb mass/cu ft
σ	surface tension, lb force/ft

Φ_g Lockhart-Martinelli parameter, dimensionless

χ two-phase-flow modulus, dimensionless

Subscripts:

av average

g gas or vapor

Hg mercury

l local

liq liquid

M momentum

mea measured

N_2 nitrogen

o inlet

S static

sat saturated

sup superheated

T total

TPF two-phase frictional

t turbulent

tt turbulent liquid, turbulent gas

v viscous

vt viscous liquid, turbulent gas

w wall

1 expulsion cylinder

2 orifice drop

3 between preheater and high flux boiler

4 Venturi inlet

5	Venturi drop
6	mercury receiver
7	reference manifold
0,12,24,36, 48,60,72	in. from condensing tube inlet

DESCRIPTION OF APPARATUS

The zero-gravity durations were obtained in a converted Navy bomber (AJ-2) flying through a portion of a ballistic path (fig. 1(a)). The aircraft and zero-gravity maneuver are discussed in appendix A. The experimental system installed in the bomb bay of the aircraft is shown in figures 1(b) and (c). Schematic drawings of a single-pass boiling and condensing system are presented in figures 1(d) and (e). The weight of the test package and related power equipment was approximately 2000 pounds. In general, the system consisted of a mercury-expulsion and liquid-flow-measuring system, a mercury preheater, a high flux boiler, a main boiler, a vapor-flow-measuring Venturi, a horizontal condensing tube, and a mercury receiver for collecting the condensed mercury. The condenser was cooled by gaseous nitrogen flowing from two diametrically opposed manifolds located above and below the condenser tube.

Experimental System and Components

Approximately 250 pounds of triple-distilled mercury were stored in a stainless-steel expulsion cylinder. A neoprene bladder was used in the cylinder to maintain orientation of the mercury in the container during the zero-gravity maneuver. Flow out of the cylinder, through a metering orifice, was maintained by pressurizing the gas side of the bladder with regulated gaseous nitrogen. The liquid flow rate was monitored according to observation of the pressure drop across the calibrated orifice.

Boiling was accomplished in three stages. Mercury was first passed through the preheater, which was designed to raise the liquid temperature to the saturation point. This unit consisted of 5 feet of stainless-steel tubing coiled around and brazed to a 1500-watt electric heater. Nucleate boiling was accomplished in a high-heat-flux unit consisting of stainless-steel tubing brazed into an electrically heated copper block. The vapor quality at the exit of this unit was about 25 percent, and the operating power was approximately 2800 watts. The 25-percent quality vapor was then passed into the main boiler that supplied the heat needed to raise the quality into the 90-percent region. This unit was a resistance heater in which the power was applied directly to the tubing that formed the mercury flow passage. Vapor was passed from the tubing into a plenum chamber that was partly filled with stainless-steel cuttings to minimize liquid carryover. The average operating power of this unit was about 9000 watts and was controlled by a thermostatic on-off control unit.

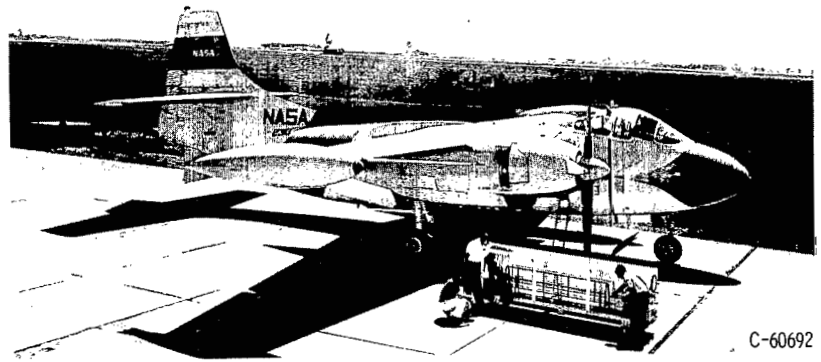

(a) AJ-2 converted Navy bomber.

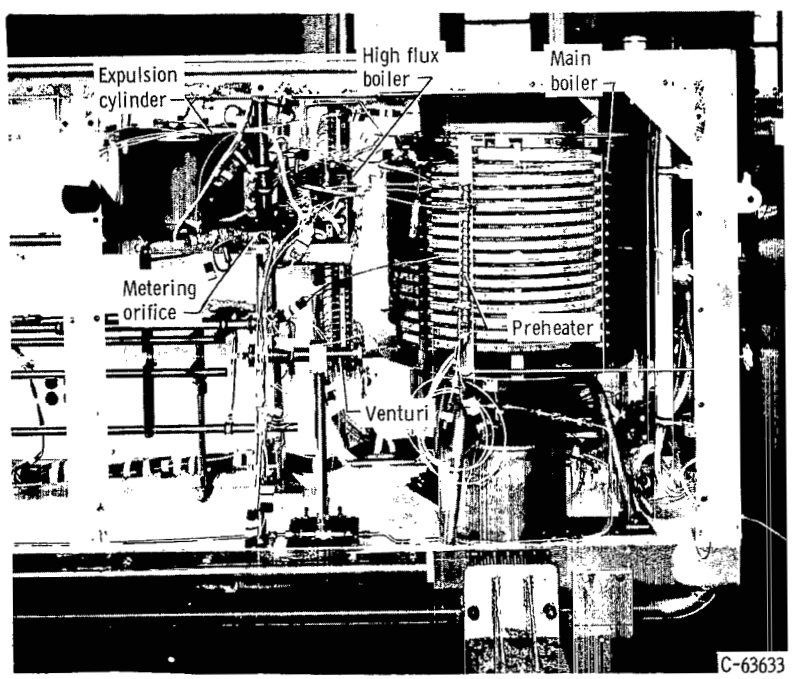

(b) Experimental package installed in aircraft (boiler end).

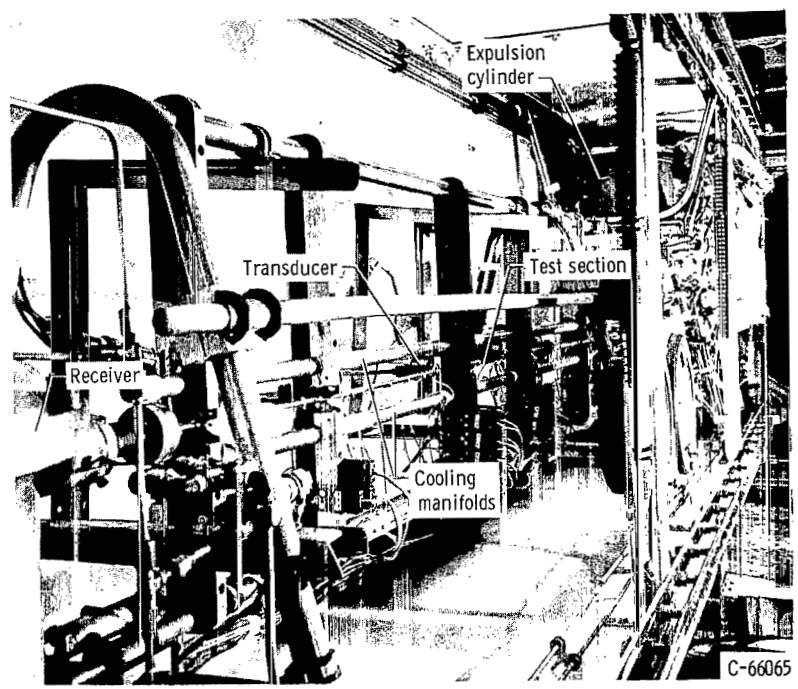

(c) Experimental package installed in aircraft (receiver end).

Figure 1. - Zero-gravity flight facility.

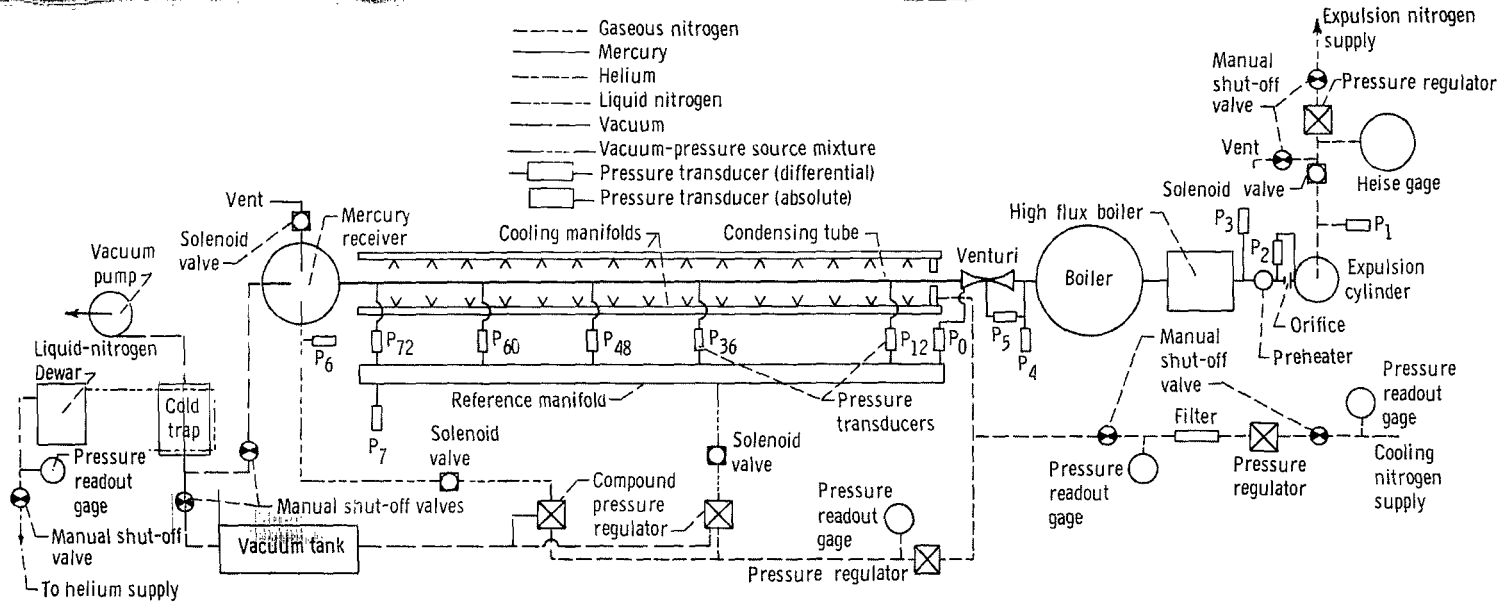

(d) Schematic drawing of system.

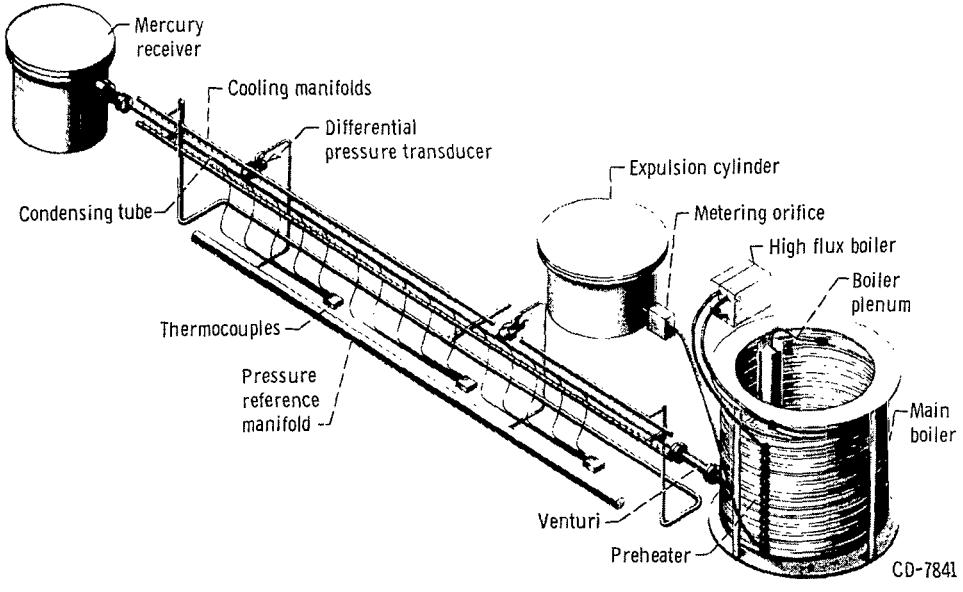

(e) Schematic drawing of components.

Figure 1. - Concluded.

The flow of mercury vapor into the condensing tube was measured by a Venturi with a throat diameter of 0.277 inch and an exit diameter equal to the condenser inlet diameter. The condenser was an 87-inch-long (type 304) stainless-steel tube (0.311 in. i.d. by 0.032-in.-thick wall) with six pressure taps located at 1-foot intervals starting 12 inches from the tube inlet. The exit of the condenser was fitted with a 1/16-inch-diameter orifice to damp out oscillations in the tube.

The mercury receiver was a stainless-steel cylinder baffled on the inside to minimize mercury movement during the zero-gravity maneuver. Receiver operating pressure was maintained at about 15 pounds per square inch absolute by a nitrogen gas pressure regulator.

Instrumentation

All temperature and pressure data needed for analysis were recorded on two 24-channel oscillographs. The accelerations generated along the three axes of the aircraft (longitudinal, lateral, and vertical) were sensed by accelerometers located in the bomb bay near the geometric center of the experiment. The gravity levels experienced here were relayed to readout equipment on the pilot's control panel and were used for aircraft control throughout the maneuver. The same gravity levels were recorded on the pressure oscillograph so that a direct comparison with system pressures could be made. The oscillograph trace illustrated the time history of the zero-gravity maneuver starting from pullup to pullout (see appendix A). About 4 to 5 seconds of the trajectory were required to damp out pressure oscillations induced by the pullup maneuver.

Stainless-steel inductance-type pressure transducers, capable of operating in a mercury environment up to 900° F, were used to measure condenser tube pressure drop, Venturi absolute pressure, and Venturi pressure drop. Low-temperature transducers were used at all other locations in the system. Each transducer in direct contact with mercury was mounted with its core axis parallel to the lateral axis of the aircraft to minimize the effects of the zero-gravity maneuver.

Temperatures throughout the system were measured by the Instrument Society of America (I.S.A.) calibration K Chromel-Alumel thermocouples. A shielded sheathed thermocouple was immersed in the mercury vapor stream in the Venturi. Thermocouples were spot-welded to the outside tube wall to determine the location of the interface. This was easily determined since the tube wall temperature decreased sharply in the liquid vapor interface region of the tube.

A second method of interface location was also used that consisted of small metal pins that projected into the condensing tube flow passage at assigned locations and were insulated electrically from the tube wall (fig. 2). Liquid mercury shorted the pins to the tube wall and activated small lights on the control panel.

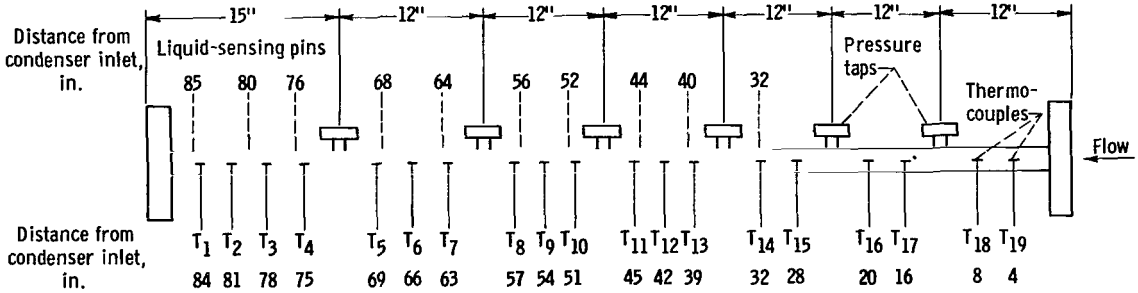

Figure 2. - Schematic diagram of test section (3/8 in. o.d. by 0.032 in. wall stainless-steel tube).

Procedure

Data were acquired in the following manner: Initially, all 1-g data points were taken on the ground with the system mounted in the aircraft and the condensing tube leveled; the same flow conditions were then repeated in zero gravity and the results compared. Later in the program a better comparison was obtained by recording the 1-g data points in the aircraft while in level flight, and the zero-gravity points immediately after without changing conditions. The aircraft accelerometers were zeroed with the condenser tube leveled to ensure good 1-g data while in flight. The data taken by both methods are presented in tables I to III.

System operating procedure was identical for both ground and flight testing. Before initiating flow through the system, the mercury system was evacuated to 60 microns of mercury, and the mercury heaters were brought to operating temperatures. Startup mass flow was set at 0.03 pound per second, and mercury vapor was allowed to purge the system for approximately 5 minutes to remove remaining noncondensables from the lines. The receiver pressure was increased to a constant value (between 14 and 15 psia). After purging, the gaseous nitrogen cooling flow was regulated to locate the interface 45 to 70 inches from the condenser inlet. Data were recorded for mercury mass flow rates of 0.025 to 0.05 pound per second, and for condenser inlet vapor temperatures corresponding to approximately 300° F of superheat. Because of liquid carryover, the superheat was necessary in this system to ensure vapor inlet quality greater than 90 percent. Data points were repeated on different days to determine test reproducibility.

Prior to every flight, a complete calibration of pressure and temperature instrumentation was carried out (appendix B).

METHOD OF ANALYSIS

Flow Regime

To analyze two-phase flow, the condenser flow regime (liquid drop distribution) must be established. The flow regime will depend on whether or not the mercury condensate wets the tube surface. The investigation reported herein is concerned with the difference between 1-g and zero-gravity pressure losses for

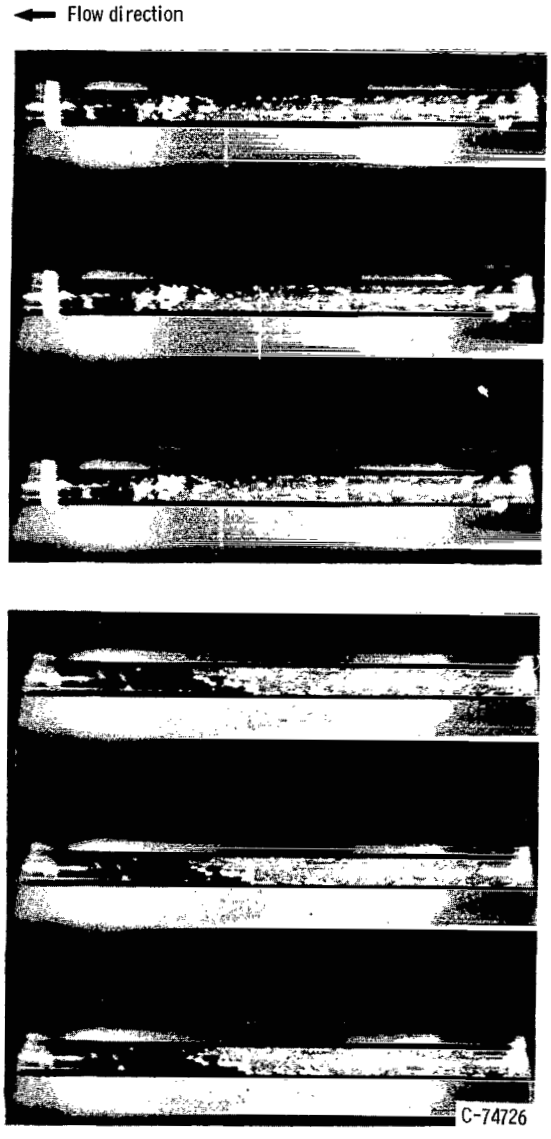

Figure 3. - Flow configurations at interface location for 1-g and zero-gravity mercury condensation (3/8 in. o.d. glass tube).

nonwetting (dropwise) condensing flow. Previous high-speed photographic studies of mercury condensing at Lewis Research Center indicate differences in the flow characteristics at the interface in 1-g and zero-gravity environments (fig. 3). Under 1-g conditions, droplet runoff was observed down the tube wall resulting in liquid accumulation in the bottom of the tube particularly in the low-velocity region. Under zero-gravity conditions, the liquid droplets are uniformly distributed around the circumference of the tube and in the vapor stream. The vapor-liquid interface in both cases is quite turbulent due to liquid impingement but basically stable position wise. In general, the droplets were observed to form on the tube inner surface, travel along the wall, increasing in size due to their coalescing with stationery droplets in their path, and in some cases being swept into the vapor stream. For high condenser inlet velocities (250 ft/sec) the entrained drops become very small and approach what is called a fog or mist flow pattern.

The three factors contributing to static pressure change of a two-phase flow in a condenser tube are the wall friction, the droplet drag, and the momentum decrease due to heat rejection. Droplets condensing on the wall would be expected to affect the roughness of tube wall surface, which would, in turn, affect the frictional pressure drop. The frictional pressure drop is also influenced by the number and the size of drops being entrained in the vapor stream and by the droplet velocity. In the condensing process, the decrease of vapor quality due to heat rejection is accompanied by a corresponding progressive reduction in vapor velocity, approaching zero at the liquid-vapor interface. This decrease in velocity from the inlet of the condenser to the interface, due to heat rejection, contributes a static pressure rise.

Determination of Heat Flux

The local frictional pressure gradient was determined by correcting the measured local pressure gradient for the momentum pressure gradient. To calculate the momentum pressure gradient, the local heat flux must be determined to establish the change in quality along the condensing tube. The local overall heat transfer coefficient (from mercury saturation temperature to the nitrogen coolant) is made up of the combined wall, mercury, and nitrogen resistances:

$$\frac{1}{UA} = R_w + R_{Hg} + R_{N_2} \tag{1a}$$

$$\frac{1}{U} = \frac{t_w D}{k(D + t_w)} + \frac{1}{h_{Hg}} + \frac{1}{h_{N_2}} \frac{D}{(D + 2t_w)} \tag{1b}$$

For a uniformly convection-cooled tube, the combined wall and cooling side resistance is constant for a given operating condition. Because the cooling gas side heat-transfer coefficient is two to three orders of magnitude lower than the mercury side condensing coefficient, the overall heat-transfer coefficient is insensitive to changes of the mercury side coefficient. Thus, for a constant cooling gas flow rate uniformly distributed along the tube length, the heat flux is uniform (from mercury saturation temperature to the nitrogen coolant) and results in a linear variation of quality along the tube length. A uniform cooling rate was provided by gaseous nitrogen flowing through 0.052-inch holes every 3/4 inch along the diametrically opposed manifolds.

But, for the test conditions considered, there existed approximately 300° F superheat at the inlet of the condenser, which contributes 6 percent of the average heat flux. Previous photographic studies of nonwetting condensation in glass tubes indicate that condensing begins very near the tube inlet. References 8 and 9 indicate that it is not necessary that the entire mass of superheated steam be cooled to the saturation temperature to initiate the condensation. Both Jakob and Kutateladze assert that a superheated vapor core can exist with condensing on the tube surface. From these considerations, it is surmised that the superheated vapor core (only 6 percent of the average heat flux) is distributed along the condensing tube resulting in a near-uniform heat flux. Considering the other extreme and assuming that no condensing takes place until all the superheat is removed change the effective

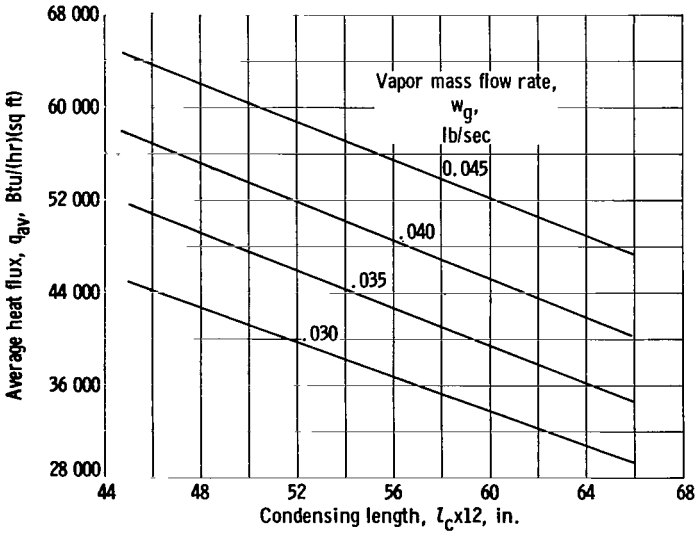

Figure 4. - Variation of average heat flux with condensing length.

condensing length by approximately 9 inches. This results in an approximate maximum deviation of 5 percent from a uniform heat flux (linear variation of velocity) and only 10 percent change in the two-phase frictional pressure drop. Thus, the assumption of a uniform heat flux is reasonable.

The average heat flux for the range of flow rates and condensing lengths investigated is presented in figure 4. Examination of the figure indicates the average heat flux ranged between 30 000 and 65 000 Btu per hour per square foot. The average heat flux is expressed as

$$q_{av} = \frac{7200 w_g \left[h_{fg} + c_p (T_{sup} - T_{sat}) \right]}{\pi D l_c} \tag{2}$$

Determination of Inlet Quality

The total flow rate for two-phase flow through an orifice meter can be determined from equation (5) of reference 10. After algebraic manipulation the equation becomes

$$x + C \sqrt{\frac{\rho_g}{\rho_{liq}}} (1 - x) = \frac{C_1 \sqrt{\Delta P_{TPF} \rho_g}}{w_T} \tag{3}$$

where C and C_1 are constants. Because of the low-vapor to liquid-density ratio for mercury, the second term of the preceding equation can be neglected for the high qualities considered. For qualities of 90 percent and above, the two-phase pressure drop is due to vapor only because the contribution of liquid carryover on the measured pressure drop is small and can be neglected. From the preceding equation the quality is expressed as the ratio of the vapor flow rate out of the boiler to the liquid flow rate into the boiler:

$$x = \frac{w_g}{w_T}$$

The liquid flow rate was determined from the pressure drop ΔP_2 across a calibrated orifice (see fig. 1(d)). Boiler performance data indicated no liquid holdup in the boiler. With steady flow assumed, the flow rate of the superheated mercury vapor into the condensing tube was determined from the density of the superheated vapor and the measured pressure drop through a Venturi. The vapor flow rate was calculated from the following equation for compressible flow through a Venturi (ref. 11)

$$w_g = A_2 K E Y \sqrt{2 g_c \Delta P_{mea} \rho_g} \tag{4}$$

where

A_2 cross-sectional area of throat, sq ft

K flow coefficient, dimensionless

E thermal expansion factor, dimensionless

Y adiabatic expansion factor, dimensionless

The density ρ_g is determined from the temperature of the superheated vapor and saturation pressure of the mercury vapor in the throat of the Venturi.

EXPERIMENTAL RESULTS

The experimental data are given in tables I to III. The data in table I were obtained on the ground with the experimental package installed in the aircraft. The data in table II were obtained in the aircraft by flying repeated zero-gravity maneuvers. The numbers designate trajectories while the letters A, B, and C designate a point during the early, middle, and late portions of the zero-gravity trajectory, respectively.

The condenser inlet pressure P_o for the first 28 trajectories presented in table II, was calculated from the Venturi inlet pressure and the Venturi pressure recovery. The pressure recovery was determined from previous 1-g data (table I) at the same flow rate.

The absolute local pressures along the test section are presented along with the mercury vapor stream temperature in the Venturi (approximate tube inlet temperature). The locations of the absolute pressure stations are identified by the subscripts to P, which denote the distance from the inlet of the tube. The position of the liquid-vapor interface is given as the distance from the condenser inlet. The calculated flow rates of the mercury liquid entering the boiler, the vapor flow rate out of the boiler, and the tube inlet quality are tabulated.

DISCUSSION OF RESULTS

Measured Local and Overall Pressure Drop

The typical local-static-pressure-drop distributions presented in figure 5 (p. 14) were obtained from the difference between the absolute local pressures along the condensing tube and the inlet absolute pressure. Examination of the figure shows that the local-static pressure drop increased over the first half of the condensing length due to the high frictional pressure losses resulting from the high vapor velocities and increased effective wall roughness caused by drop formation. In the last half of the condensing length, however, the pressure rise due to momentum decrease exceeds the frictional pressure loss. This results in a net decrease in local-static pressure drop, and consequently, a relatively small overall static pressure drop. For the curves shown in figure 5, the percentage difference of the inlet dynamic pressure ($\rho_o u_o^2/2g_c$) was less than 5 percent. With the inlet conditions approximately the same there was no discernible difference between the 1-g and zero-gravity static-pressure-drop distributions.

The effect of gravity on the measured overall (inlet to interface) static pressure drop for various flow rates, inlet pressures, and inlet temperatures is presented in figure 6 (p. 15). The flow rates (0.028 and 0.046 lb mass/sec)

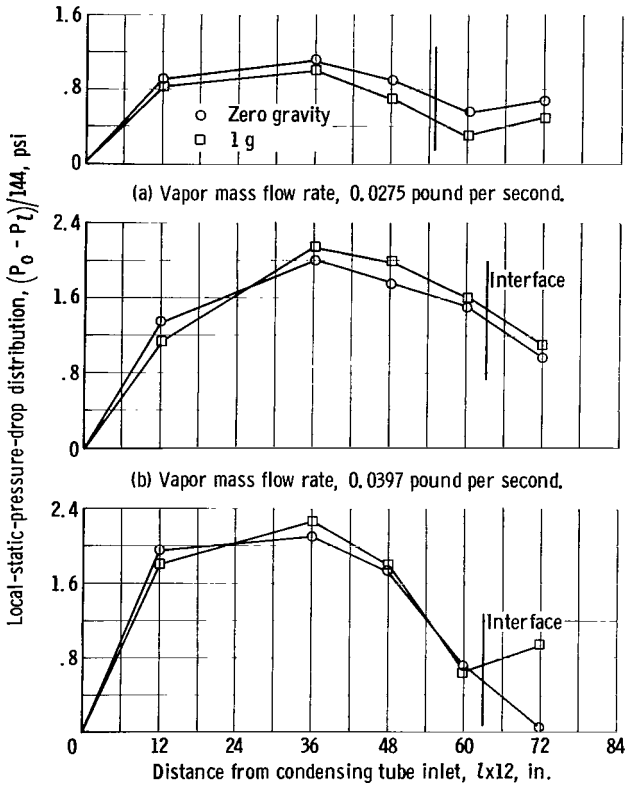

Figure 5. - Typical local-static-pressure-drop distributions along condensing tube for 1-g and zero-gravity environments.

were chosen for discussion because sufficiently comparable data were obtained at these flow rates. For both sets of data, the overall pressure drop increases with condensing length as a result of the increase of frictional loss with tube length. The overall static pressure drop varied from 0.2 to 2.2 pounds per square inch for condensing lengths from 45 to 70 inches and vapor inlet flows from 0.028 to 0.046 pound mass per second. Examination of figure 6(a) shows that most of the zero-gravity points fall above the line, while most of 1-g points fall below the line. Within the accuracy of the instrumentation, the data spread indicates little apparent difference between 1-g and zero-gravity static pressure drop at a flow rate of 0.028 pound mass per second. The gravity effect on the overall pressure drop was also negligible at a flow rate of 0.046 pound mass per second (see fig. 6(b)).

The changes in overall total pressure loss with condensing length for both 1-g and zero-gravity conditions are presented in figure 7. These plots were obtained by adding the inlet dynamic pressure to the overall static pressure drop, where the dynamic pressure in the liquid portion is negligible. The overall total pressure loss varied from 1.4 to 5.4 pounds per square inch for condensing lengths from 45 to 70 inches for the flow rates considered.

Comparison of Local-Frictional-Pressure-Drop Data with Lockhart-Martinelli Correlation

A comparison of two-phase pressure losses is often made with correlations developed by Lockhart and Martinelli for two-phase, two component, adiabatic flow. This correlation takes into account the variation of local properties along the tube. Local experimental Lockhart-Martinelli parameters for a straight tube were determined from (1) local static pressure, (2) flow rate, (3) condensing length, (4) inlet quality, (5) axial location of pressure taps (appendix C). The local-frictional pressure gradient was determined by correcting the measured local pressure gradient for the momentum pressure gradient. The change in momentum is a function of the variation in the velocity of the liquid and the gas. The slip ratio ϵ is defined as

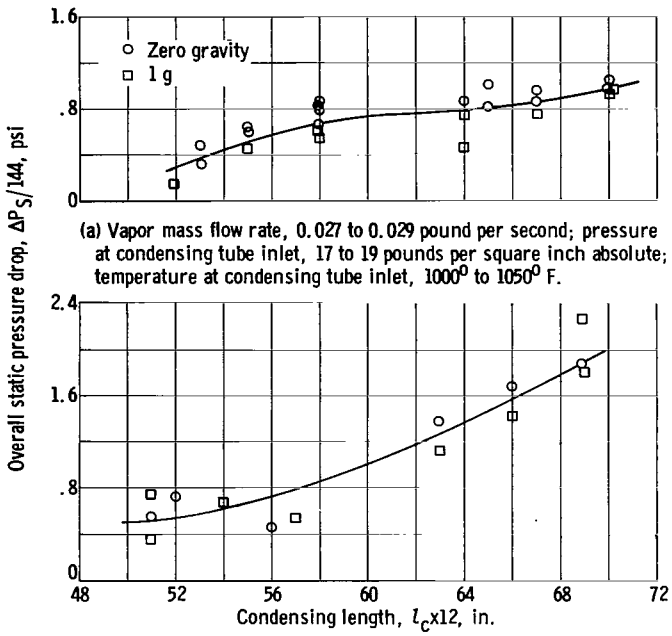

(a) Vapor mass flow rate, 0.027 to 0.029 pound per second; pressure at condensing tube inlet, 17 to 19 pounds per square inch absolute; temperature at condensing tube inlet, 1000^0 to 1050^0 F.

(b) Vapor mass flow rate, 0.045 to 0.047 pound per second; pressure at condensing tube inlet, 18.4 to 21.4 pounds per square inch absolute; temperature at condensing tube inlet, 980^0 to 1100^0 F.

Figure 6. - Effect of gravity on overall static pressure drop.

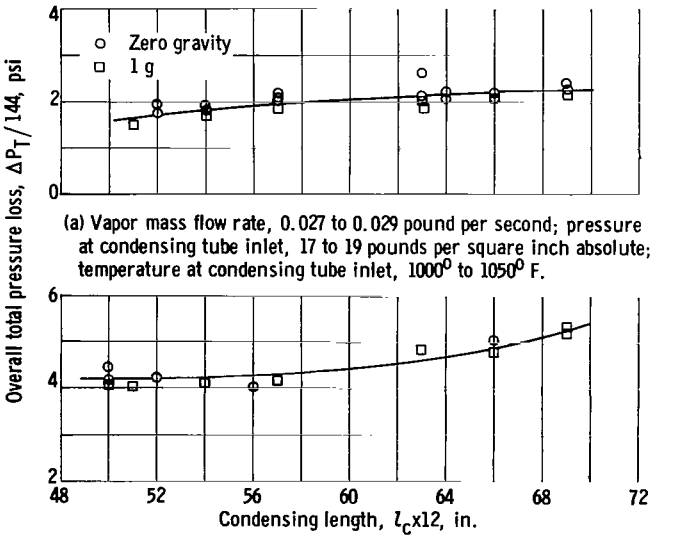

(a) Vapor mass flow rate, 0.027 to 0.029 pound per second; pressure at condensing tube inlet, 17 to 19 pounds per square inch absolute; temperature at condensing tube inlet, 1000^0 to 1050^0 F.

(b) Vapor mass flow rate, 0.045 to 0.047 pound per second; pressure at condensing tube inlet, 18.4 to 21.4 pounds per square inch absolute; temperature at condensing tube inlet, 980^0 to 1100^0 F.

Figure 7. - Effect of gravity on overall total pressure drop.

$$\epsilon = \frac{u_g - u_{liq}}{u_g}$$

Observations of nonwetting condensing flow patterns in glass tubes indicated that the predominant flow pattern for low-heat-flux mercury condensation was fine drops dispersed in the vapor stream. Similar observations are discussed in reference 7. The data spread was much less for an assumed slip ratio of zero ($u_{liq} = v_g$) than for a slip ratio of 1 ($u_{liq} = 0$). The local pressure recovery was calculated by assuming a slip ratio of zero. The derivation of the equation used to determine the pressure recovery due to momentum decrease for a slip ratio of zero is given in appendix D. The pressure losses due to the gas alone were determined from equations (E5) and (E7) of appendix E. For local values of Lockhart-Martinelli parameters, v_{liq} and μ_{liq} were considered constant and were determined by the average pressure in the tube. The determination of v_g and μ_g were based on the local saturation pressure and superheated temperature (ref. 12). A linear decrease in quality was assumed in the determination of condensing pressure drop gradients and Martinelli parameters.

The Lockhart-Martinelli correlation predicts Φ_g within ±30 percent and $(\Delta P/\Delta L)_{TPF}$ within ±70 percent for the high quality, high vapor Reynolds number region (i.e., low values of the parameter χ, fig. 8). The condensing pressure gradient Φ_g both for 1-g and zero-gravity is about 200 percent greater than predicted by Lockhart-Martinelli for the low quality region of the tube (i.e., high value of the Lockhart-Martinelli parameter χ).

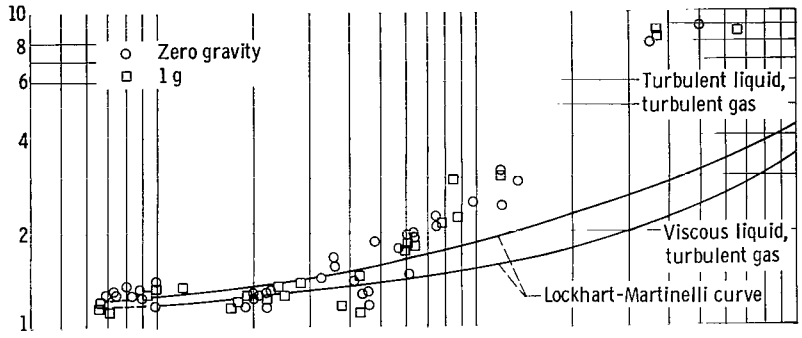

(a) Vapor mass flow rate, 0.027 to 0.029 pound per second; pressure at condensing tube inlet, 17 to 19 pounds per square inch absolute; temperature at condensing tube inlet, 1000^0 to 1050^0 F.

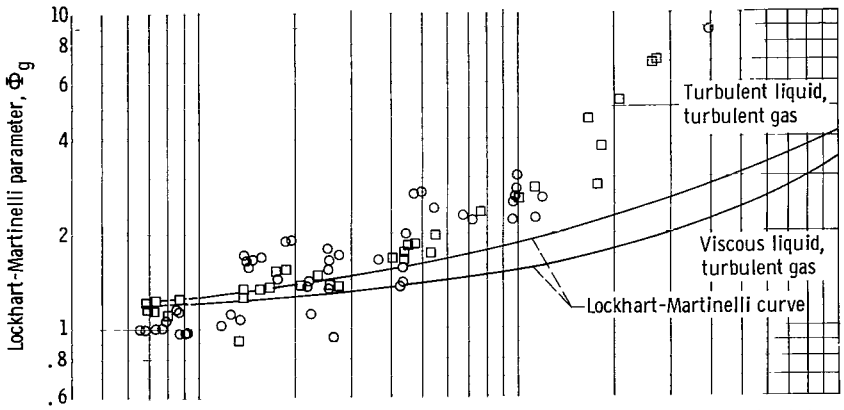

(b) Vapor mass flow rate, 0.038 to 0.040 pound per second; pressure at condensing tube inlet, 18 to 20 pounds per square inch absolute; temperature at condensing tube inlet, 1000^0 to 1100^0 F.

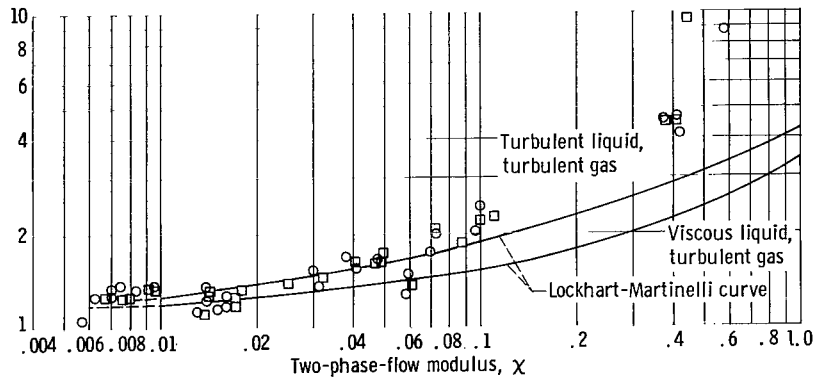

(c) Vapor mass flow rate, 0.045 to 0.047 pound per second; pressure at condensing tube inlet, 18.4 to 21.4 pounds per square inch absolute; temperature at condensing tube inlet, 980^0 to 1100^0 F.

Figure 8. - Comparison of local-frictional-pressure-drop data with Lockhart-Martinelli correlation.

This deviation indicates that it is only in the low quality region of the condenser that wall roughness and droplet drag considerations are significantly different from those assumed for the Lockhart-Martinelli flow model.

Comparison of Local-Frictional-Pressure-Drop Data with Fog-Flow Correlation

For high-velocity condensing (250 ft/sec), the entrained drop size is considered to be very small. The flow regime approaches a fog-flow condition in which the vapor and liquid are treated as single phase. The ratio of the two-phase pressure drop to that of the vapor can be expressed as a function of Weber number and quality (ref. 7). The fog-flow correlation is expressed as

$$\Phi_g^2 x^{3/4} = f\left(\frac{D\rho_g u_g^2}{2g_c\sigma_{liq}}\right) \tag{5}$$

The Weber number is a function of an experimental constant E_σ and the ratio of the tube diameter to the fog-flow diameter:

$$\frac{D\rho_g u_g^2}{2g_c\sigma_{liq}} = \frac{8E_\sigma}{\left(\frac{D}{D_m}\right)^4 - \left(\frac{D}{D_m}\right)^3} \tag{6}$$

Experiments with single mercury droplets showed the constant E_σ to have the value of 0.0464. This constant accounts for the effects of drop deformation, contact angle, and surface condition.

The fog-flow parameter $\Phi_g^2 x^{3/4}$ is expressed in terms of the ratio of the diameters

$$\Phi_g^2 x^{3/4} = \left(\frac{D}{D_m}\right)^{4.75} \tag{7}$$

where D_m is the diameter of the flow passage formed by the drops on the wall through which the fog flows. By assuming values of the ratio D/D_m, the relation between the fog-flow parameter and Weber number was obtained.

Generally, the data trend correlates with the fog-flow theory (fig. 9). The data indicate that the fog-flow parameter $\Phi_g^2 x^{3/4}$ approaches 1 for high values of the Weber number $(D\rho_g u_g^2/2g_c\sigma_{liq})$ ranging from 10 to 300. The data spread is least in the high-velocity (high-Weber-number) region of the tube that approaches the fog-flow regime. The effect of gravity on the experimental frictional pressure gradient was negligible for both the Lockhart-Martinelli and the fog-flow correlations.

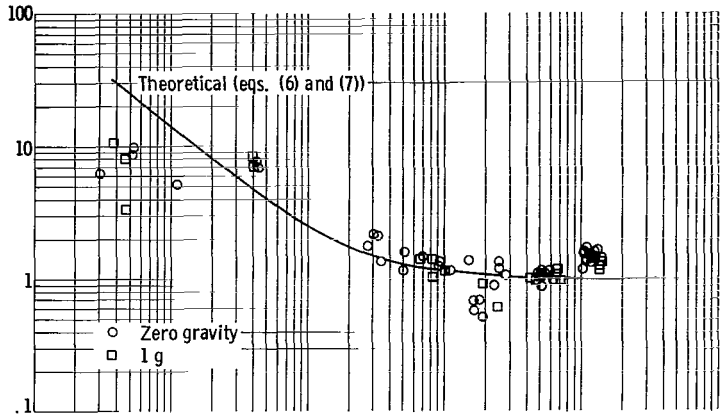

(a) Vapor mass flow rate, 0.027 to 0.029 pound per second; pressure at condensing tube inlet, 17 to 19 pounds per square inch absolute; temperature at condensing tube inlet, 1000^0 to 1050^0 F.

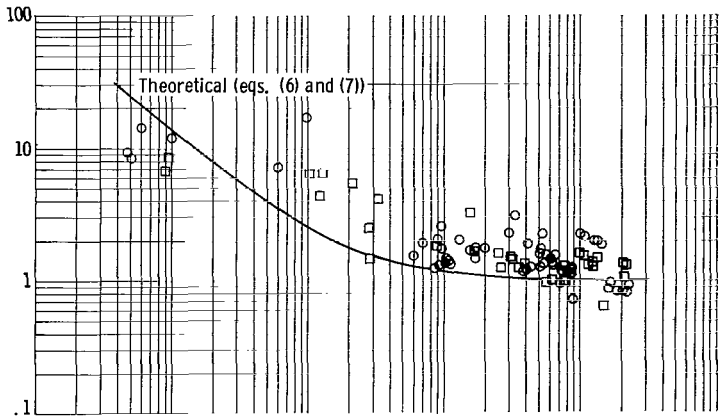

(b) Vapor mass flow rate, 0.038 to 0.040 pound per second; pressure at condensing tube inlet, 18 to 20 pounds per square inch absolute; temperature at condensing tube inlet, 1000^0 to 1100^0 F.

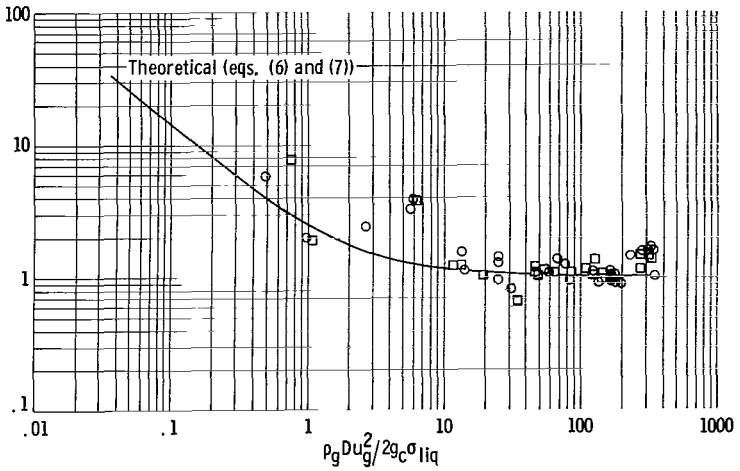

(c) Vapor mass flow rate, 0.045 to 0.047 pound per second; pressure at condensing tube inlet, 18.4 to 21.4 pounds per square inch absolute; temperature at condensing tube inlet, 980^0 to 1100^0 F.

Figure 9. - Comparison of local-frictional-pressure-drop data with fog-flow correlation.

SUMMARY OF RESULTS

An experimental study of the pressure losses of condensing mercury in a constant diameter tube in 1-g and zero-gravity environments yielded the following principal results:

1. The overall static pressure drop varied from 0.2 to 2.2 pounds per square inch, while the total pressure loss varied from 1.4 to 5.4 pounds per square inch for the condensing lengths and the mass flow rates considered.

2. The measured overall static pressure drop at flow rates of 0.028 and 0.046 pound mass per second (where sufficiently comparable data were obtained) indicated little difference between 1-g and zero-gravity pressure losses.

3. The Lockhart-Martinelli correlation predicts Φ_g within ±30 percent, $(\Delta P/\Delta L)_{TPF}$ within ±70 percent, for the high-velocity high-quality region of the condensing tube. The pressure gradients both for 1 g and zero gravity are greater than predicted by Lockhart-Martinelli for the low-quality region of the tube.

4. Generally, the data trend correlates with the fog-flow theory. The data indicate that the fog-flow parameter approaches 1 for high values of the Weber number ranging from 10 to 300. The data spread is least in the high-velocity (high-Weber-number) region of the tube that approaches the fog-flow regime.

5. For the local plots of the Lockhart-Martinelli and the fog-flow correlations, the effect of gravity was negligible.

Lewis Research Center,
National Aeronautics and Space Administration,
Cleveland, Ohio, March 11, 1965.

APPENDIX A

AJ-2 ZERO-GRAVITY FLIGHT FACILITY

by Clifford C. Crabs

The AJ-2 airplane that was used for the test flights is a converted Navy attack bomber shown previously in figure 1(a) (p. 6). The aircraft was modified to assure fuel and oil supply to the engines during the zero-gravity flights. The only other necessary modification was the addition of structures for mounting the test package semirigidly to the aircraft. Thrust for the flight was supplied by two reciprocating powerplants and one jet engine.

A typical trajectory for the Lewis AJ-2 airplane is shown in figure 10. This maneuver produces a theoretical maximum zero-gravity time, as shown in the figure, of 24 seconds. The maneuver was entered from a dive and the airplane was rotated at 400 knots true airspeed to arrive at a pitch angle of 42° with a speed of 310 knots true airspeed. Transition was made from a nominal 2-g pullup rotation to the zero-gravity condition where the aircraft was flying on a

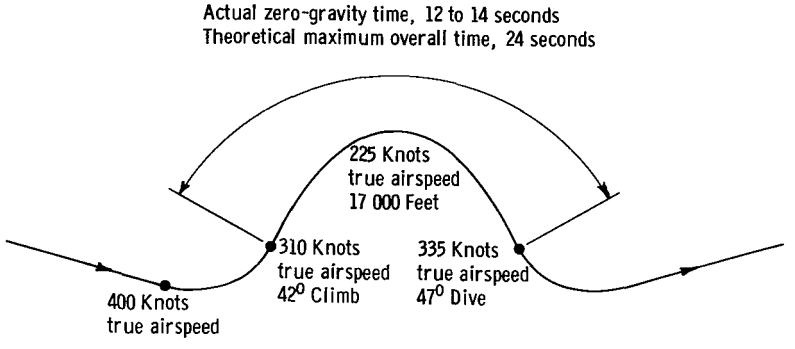

Figure 10. - Typical trajectory.

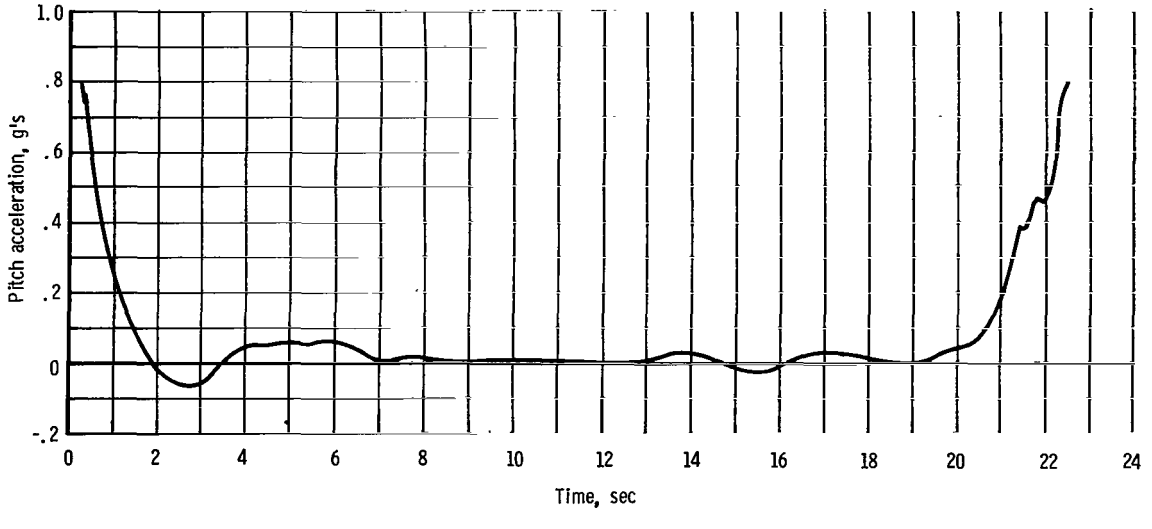

Figure 11. - Pitch acceleration during typical trajectory.

Keplerian trajectory. Approximately 5 or 6 seconds were required for transition from the pullup to the zero-gravity condition, and a similar time was required at the exit of the Keplerian curve to pullout. These transition times reduce the theoretical maximum zero-gravity time to a practical time of 12 to 14 seconds.

The zero-gravity times obtained for this study were adequate, since flow-stabilization times in the experimental system were of the order of 4 to 5 seconds.

The quality of the zero-gravity condition produced in the aircraft should be considered on the basis of the three axes of measurement; however, the lateral and longitudinal accelerations always had a better quality than the vertical acceleration. The vertical accelerations for a typical trajectory are shown in figure 11. During this maneuver, 2.5 seconds were at a level of 0.005 g or less, while 19.1 seconds were at a level less than 0.1 g.

All of the maneuvers flown during the test program were analyzed and the average zero-gravity times were computed. From these data it was shown that, for an average of 5.28 seconds per trajectory, the gravity level was within ±0.01 g and for 12.72 seconds the gravity level was within ±0.05 g.

Flights were made in a restricted airspace over Lake Erie because of the possibility of an inadvertent mercury spillage. The aircraft was monitored on radar for separation from stray aircraft and continuous radio contact was maintained with NASA Flight Operations as an added precaution. On initial flights, a "chase" aircraft was flown with the AJ-2 to observe any possible external malfunctions or system leakages.

APPENDIX B

CALIBRATION

The locations of pressure and temperature instrumentation used in the following discussion are shown in figure 2 (p. 9). The system schematic (fig. 1(d), p. 6) will also be helpful in following this discussion.

All differential pressure transducers were calibrated simultaneously by pressurizing the mercury system with gaseous nitrogen through the Venturi. The low pressure sides of the transducers were all referenced to atmospheric pressure, and a selected range of gage pressure was applied to the system. The desired oscillograph and readout gage spans were set up, and recorder runs were made over the calibration range so that transducer calibration curves could be plotted.

The absolute pressure transducers were also calibrated simultaneously by applying pressure to the entire system. In order to zero these transducers, the system was first pumped to a vacuum (1 mm). All other transducers in the system were calibrated individually.

Every high-temperature transducer was calibrated in the system at room temperature before each test run. A calibration in an oven at 500° F indicated a change in transducer output. For the high-temperature transducers in the vapor region, the operating temperature of the diaphragms was estimated to be a maximum of approximately 300° F. The change in output caused by operating at these temperatures was approximately 0.5 percent of the maximum output of the transducers and was considered sufficiently small to neglect when reducing the data.

Temperature indicators on the main control panel needed only periodic inspection for accuracy. The mercury vapor temperature was read on one indicator, and condensing tube wall temperatures, utilizing a selector switch for rapid scanning, were read on a similar indicator. Other system temperatures, used mainly for system operation and control, were read out either on controllers or on the temperature oscillograph.

APPENDIX C

MARTINELLI'S PARAMETERS

Martinelli proposed the ratio of two-phase frictional pressure drop to the frictional pressure drop of the gas alone. This is expressed as

$$\Phi_g^2 = \frac{\left(\frac{\Delta P}{\Delta L}\right)_{TPF}}{\left(\frac{\Delta P}{\Delta L}\right)_g} \tag{C1}$$

where Φ_g is a function of the variable χ, the ratio of the frictional pressure drop of the liquid to that of the gas. This is expressed as

$$\chi^2 = \frac{\left(\frac{\Delta P}{\Delta L}\right)_{liq}}{\left(\frac{\Delta P}{\Delta L}\right)_g} \tag{C2}$$

The ratio in equation (C2) can be calculated from the fluid properties and mass flow rates of the liquid and the gas. The general form of the Martinelli flow parameter is

$$\chi^2 = \frac{C_{liq}}{C_g} \frac{w_{liq}^2}{w_g^2} \frac{v_{liq}}{v_g} \frac{\left(Re_g\right)^m}{\left(Re_{liq}\right)^n} \tag{C3}$$

The coefficients C_{liq} and C_g and the exponents m and n depend on the particular flow regime being considered and are given in reference 1.

The two parameters most appropriately suited for two-phase flow considered here are

$$\chi_{vt} = \left(\frac{16}{0.046} \frac{v_{liq}}{v_g} \frac{\mu_{liq}}{\mu_g} \frac{w_{liq}}{w_g}\right)^{0.5} Re_g^{-0.4} \tag{C4a}$$

$$\chi_{tt} = \left(\frac{w_{liq}}{w_g}\right)^{0.9} \left(\frac{v_{liq}}{v_g}\right)^{0.5} \left(\frac{\mu_{liq}}{\mu_g}\right)^{0.1} \tag{C4b}$$

Correcting for momentum effects gives the ratio of the frictional two-phase pressure drop to the gas-phase pressure drop:

$$\Phi_g^2 = \frac{\int_{l_1}^{l_2} \left[\left(\frac{\Delta P}{\Delta L}\right)_{mea} + \left(\frac{\Delta P}{\Delta L}\right)_M\right] dL}{\left(\frac{\Delta P}{\Delta L}\right)_g} \tag{C5}$$

where in this case l_2 and l_1 refer to points at one pressure tap and its preceding pressure tap, respectively.

APPENDIX D

PRESSURE RECOVERY

In the condensing process, the change in momentum of the liquid and the gas acts in the opposite direction to the two-phase frictional pressure drop. The general expression for the change in momentum is

$$-dPA_T = \frac{d(w_g u_g)}{g_c} + \frac{d(w_{liq} u_{liq})}{g_c} \tag{D1}$$

Expanding equation (D1) yields

$$-dPA_T g_c = w_g\, du_g + u_g\, dw_g + w_{liq}\, du_{liq} + u_{liq}\, dw_{liq} \tag{D2}$$

however,

$$\left.\begin{aligned} w_g &= w_T x & dw_g &= w_T\, dx \\ u_g &= u_o x & du_g &= u_o\, dx \\ w_{liq} &= w_T(1 - x) & dw_{liq} &= -w_T\, dx \end{aligned}\right\} \tag{D3}$$

The local velocity of the liquid cannot be obtained without introducing the area of the tube occupied by the liquid, unless some relation between the velocity of the liquid and gas is known. The slip ratio is defined as

$$\epsilon = \frac{u_g - u_{liq}}{u_g}$$

The local pressure recovery thus changes for various slip ratios. For high-velocity dropwise condensation, the drops are accelerated very rapidly to the velocity of the gas, thus approaching a slip ratio of zero. Then

$$\left.\begin{aligned} u_{liq} &= u_g \\ du_{liq} &= du_g \end{aligned}\right\} \tag{D4}$$

By use of equations (D2) to (D4), the pressure rise for a slip ratio of zero becomes

$$-dP_M = \frac{G_T u_o}{g_c}\, dx \tag{D5}$$

Now,

$$u_o = \frac{G_T}{\rho_g} \tag{D6}$$

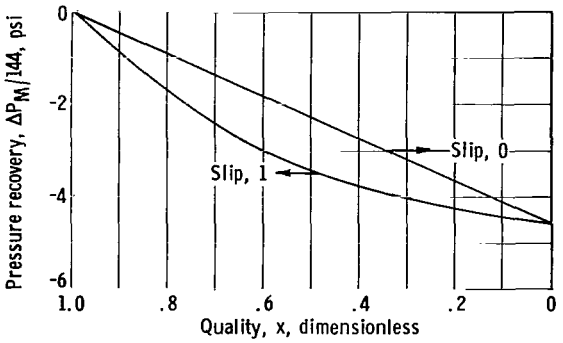

Figure 12. - Comparison of local pressure recovery for slip ratios of 0 and 1 against quality (mass flow rate, 0.04 lb/sec).

Thus,

$$-dP_M = \frac{G_T^2}{\rho_g g_c} dx \qquad (D7)$$

If the velocity of liquid is neglected (slip equals 1), the pressure rise due to momentum decrease is determined by the first term of equation (D1):

$$-dP_M = \frac{2G_T^2 x}{\rho_g g_c} dx \qquad (D8)$$

The comparison of pressure recovery for slip ratios of zero and one against quality along the condenser tube is shown in figure 12. The overall pressure recovery is shown to be independent of an assumed slip ratio, but the local pressure rise due to momentum decrease is greater for a slip ratio of one than for a slip ratio of zero for qualities $0 < \chi < 1$. This is due to the pressure loss required to accelerate the liquid to the vapor velocity for a slip condition of zero.

APPENDIX E

GAS PRESSURE DROP

The Fanning equation for steady flow in uniform circular pipes is used to determine the frictional pressure drop due to the gas phase alone. It is expressed as

$$\left(\frac{\Delta P}{\Delta L}\right)_g = \frac{4f\rho u^2}{D2g_c} \tag{E1}$$

where, for uniform heat flux along the condensing length,

$$G_g = \frac{4w_T x}{\pi D^2} = \frac{4w_T x_o\left(1 - \frac{l}{l_c}\right)}{\pi D^2} \tag{E2}$$

The friction factor for turbulent flow in a smooth pipe is expressed as (ref. 13),

$$f_t = \frac{0.046}{Re_g^{0.2}} \tag{E3}$$

By use of equations (E1) to (E3), the frictional pressure drop in turbulent flow is expressed as

$$\left(\frac{\Delta P}{\Delta L}\right)_{gt} = \frac{2(0.046)(w_T x_o)^2\left(1 - \frac{l}{l_c}\right)^2}{g_c(Re_g)^{0.2}\left(\frac{\pi}{4}\right)^2 D^5 \rho_g} \tag{E4}$$

Substituting l in terms of quality in equation (E4) yields

$$dP_{gt} = -\frac{0.092\ \mu_g^{0.2} G_T^{1.8} l_c x^{1.8}}{D^{1.2}\rho_g g_c x_o}\ dx \tag{E5}$$

The friction factor for viscous flow for a Reynolds number less than 2000 is

$$f_v = \frac{16}{Re_g} \tag{E6}$$

The frictional pressure drop for viscous flow becomes

$$\left(\frac{\Delta P}{\Delta L}\right)_{gv} = \frac{32\left(w_T x_o\right)^2 1 - \left(\frac{l}{l_c}\right)^2}{Re_g\left(\frac{\pi}{4}\right)^2 D^5 \rho_g g_c} \tag{E7}$$

REFERENCES

1. Lockhart, R. W.; and Martinelli, R. C.: Proposed Correlation of Data for Isothermal Two-Phase, Two-Component Flow in Pipes. Chem. Eng. Prog., vol. 45, no. 1, 1949, pp. 39-48.

2. Baroczy, C. J.; and Sanders, V. D.: Pressure Drop for Flowing Vapors Condensing in a Straight Horizontal Tube. Rept. No., NAA-SR-6333, Atomics Int., North Am. Aviation, Inc., June 1, 1961.

3. Hays, L.: Investigation of Condensers Applicable to Space Power Systems. Pt. 1. Direct Condensers. Rept. No. 1588, Electro-Optical Systems, Inc., Aug. 15, 1962.

4. Kiraly, R. J.; and Koestel, A.: The SNAP-II Power Conversion System Topical Report No. 8. Mercury Condensing Research Studies. Rept. No. ER-4442, Thompson Ramo Wooldridge, Inc., May 31, 1961.

5. Jaenke, C. T.; Koestel, A.; and Reitz, J. G.: The SNAP-II Power Conversion System Topical Report No. 13. Orbital Force Field Boiling and Condensing Experiment (Offbace). Rept. No. Er-4670, Thompson Ramo Wooldridge, Inc., Oct. 1962.

6. Gido, R. G.; and Koestel, A.: Mercury Wetting and Non-Wetting Condensing Research. Prog. Rept. No. 3, Rept. No. ER-5214, Thompson Ramo Wooldridge, Inc., Jan. 1963.

7. Koestel, Alfred; Gutstein, Martin U.; and Wainwright, Robert T.: Study of Wetting and Nonwetting Mercury Condensing Pressure Drops. NASA TN D-2514, 1964.

8. Kutateladze, S. S. (S. J. Rimshaw, trans.): Heat Transfer in Condensation and Boiling. Rept. No. TR-3770, AEC, pp. 53-60.

9. Jakob, Max: Heat Transfer in Evaporation and Condensation, II. Mech. Eng., vol. 58, No. 11, Nov. 1936, pp. 729-739.

10. Murdock, J. W.: Two-Phase Flow Measurement with Orifices. J. Basic Eng. (ASME trans.), ser. D, vol. 84, no. 2, Dec. 1962, pp. 419-433.

11. Anon.: Power Test Codes - Instruments and Apparatus. ASME, 1959, pt. 5, ch. 4.

12. Weatherford, W. D., Jr.; Tyler, J. C.; and Ku, P. M.: Properties of Inorganic Energy-Conversion and Heat-Transfer Fluids for Space Applications. Rept. No. 61-96, WADD, Nov. 1961.

13. McAdams, W. H.: Heat Transmission. Third ed., McGraw-Hill Book Co., Inc., 1954.

TABLE I. - 1-g GROUND DATA

Point identification	Condensing length, l_c, in.	Liquid mass flow rate, w_{liq}, lb/sec	Vapor mass flow rate, w_g, lb/sec	Inlet quality, x_o	Static pressure, psia							Temperature at condensing tube inlet, T_o, °F
					P_0	P_{12}	P_{24}	P_{36}	P_{48}	P_{60}	P_{72}	
1	68	0.0408	0.0404	0.99	18.40	17.15	16.23	15.85	15.75	16.10	16.90	1020
2	66	.0402	.0392	.98	18.98	17.25	16.30	16.25	16.15	16.30	17.20	1020
3	63	.0408	.0393	.96	18.95	17.35	16.30	16.45	16.60	16.98	17.50	1022
4	63	.041	.04	.97	19.55	18.40	17.60	17.40	17.55	17.95	18.45	1024
5	63	.041	.04	.97	19.10	17.85	17.05	16.90	16.95	17.35	17.65	1031
6	63	.041	.0395	.96	19.15	18.40	17.15	16.95	17.15	17.55	18.10	1040
7	56	.0403	.0397	.99	18.90	17.70	17.15	17.15	17.40	18.05	18.25	1043
8	55	.0402	.0396	.99	18.90	17.85	17.20	17.25	17.50	18.15	18.30	1048
9	69	.04	.0399	1.00	18.50	18.30	17.20	16.75	16.55	17.05	17.10	1020
10	66	.04	.0399	1.00	17.95	16.85	15.85	15.50	15.45	16.00	16.47	1030
11	47	.0408	.0384	.94	18.72	17.75	17.35	17.50	18.05	18.40	18.50	1062
12	46	.04	.0387	.97	18.19	17.49	16.89	17.27	17.79	18.14	18.24	1078
13	60	.04	.0376	.94	19.86	18.78	17.88	17.68	17.78	18.08	18.68	1080
14	45	.04	.0392	.98	18.38	17.55	17.08	17.42	17.89	18.24	18.39	1078
15	45	.0408	.0381	.93	18.19	17.34	16.87	17.18	17.64	17.98	18.13	1078
16	45	.0408	.0384	.94	18.22	17.40	16.84	17.20	17.67	18.03	18.15	1080
17	46	.04	.0388	.97	18.63	17.78	17.27	17.53	18.04	18.46	18.55	1065
18	46	.0401	.0392	.98	18.67	17.87	17.37	17.77	18.13	18.55	18.63	1065
19	47	.0397	.0396	.99	18.22	17.28	16.97	17.28	17.70	18.09	18.34	1058
20	55	.0402	.0398	.99	19.42	18.31	17.60	17.72	18.01	18.57	18.76	1048
21	55	.0402	.0384	.96	18.93	18.21	17.71	17.88	17.51	18.13	18.29	1050
22	64	.04	.0388	.97	19.79	17.62	17.62	17.32	17.37	17.69	18.31	1088
23	60	.04	.0390	.98	18.97	17.92	17.30	17.32	17.56	18.18	18.30	1048
24	60	.04	.0382	.96	19.69	18.67	17.76	17.51	17.57	18.02	18.51	1085
25	65	.042	.0384	.92	20.02	18.86	17.84	17.49	17.46	17.78	18.47	1100
26	67	.0328	.0317	.97	17.23	16.62	16.09	15.35	15.44	15.45	15.90	1078
27	65	.032	.031	.97	17.00	16.40	15.69	15.17	15.29	15.47	15.68	1105
28	66	.0321	.0321	1.00	17.73	17.09	16.40	15.66	15.73	15.73	16.23	1082
29	66	.0322	.0322	1.00	17.84	17.30	16.55	15.88	15.93	15.98	16.42	1082
30	45	.0326	.032	.99	16.43	16.01	15.75	15.61	16.08	15.98	16.38	1082
31	45	.0323	.0322	1.00	16.35	15.85	15.58	15.29	15.73	15.74	16.15	1082
32	45	.0339	.0325	.96	16.51	16.00	15.87	15.45	15.93	15.88	16.20	1085
33	45	.0322	.0321	1.00	17.12	16.70	16.32	16.08	16.55	16.51	17.08	1088
34	45	.033	.0322	.98	17.23	16.91	16.52	16.21	16.74	16.68	17.19	1088
35	44	.0345	.0342	.99	16.43	16.14	15.84	15.69	16.19	16.05	16.25	1085
36	44	.0339	.0332	.98	16.39	16.02	15.61	15.50	15.95	15.78	16.27	1095
37	44	.0347	.0332	.96	16.35	15.96	15.76	15.63	16.04	15.85	16.43	1088
38	51	.030	.030	1.00	17.01	16.54	16.20	16.42	16.34	16.28	16.80	1085
39	54	.031	.0296	.96	16.57	16.33	15.83	15.53	15.84	15.89	16.26	1105
40	51	.0316	.0282	.90	16.88	16.70	16.15	15.83	16.13	16.12	16.48	1105
41	51	.0316	.0312	.99	16.89	16.73	16.12	15.77	16.40	16.09	16.64	1082
42	52	.0317	.0316	1.00	17.02	16.83	16.27	15.94	16.29	16.23	16.82	1082
43	54	.0308	.0307	1.00	17.20	16.90	16.24	15.96	16.32	16.32	16.76	1085
44	54	.0316	.0302	.96	16.95	16.65	15.98	15.65	15.95	15.90	16.53	1105
45	54	.0314	.0302	.96	17.66	17.46	16.77	16.48	16.81	16.82	17.33	1105
46	54	.0311	.0311	1.00	16.97	16.76	16.10	15.78	16.17	16.15	16.65	1082
47	54	.0317	.0308	.97	16.78	16.58	15.96	15.80	16.08	16.08	16.58	1105
48	54	.0318	.0306	.96	16.70	16.39	15.78	15.47	15.80	15.79	16.30	1085
49	66	.0308	.0308	1.00	17.97	17.57	16.86	16.45	16.05	16.27	16.68	1088
50	67	.0316	.0305	.96	17.22	16.91	16.53	15.88	15.30	15.28	15.90	1085
51	66	.0307	.0307	1.00	18.02	17.65	16.99	16.55	16.14	16.35	16.81	1085
52	67	.0319	.0310	.97	17.99	17.52	16.85	16.22	16.23	16.24	16.68	1085
53	66	.0307	.0307	1.00	18.19	17.96	17.18	16.55	16.60	16.65	17.08	1082
54	67	.0311	.0297	.96	17.59	17.04	16.40	15.82	15.92	15.85	16.28	1082
55	68	.0303	.0303	1.00	18.48	18.12	17.42	16.75	16.82	16.83	17.25	1082
56	68	.0301	.0301	1.00	18.05	17.71	17.09	16.39	16.44	16.56	16.88	1082
57	68	.0307	.0307	1.00	17.95	17.50	16.82	16.23	16.29	16.33	16.76	1082

TABLE II. - ZERO-GRAVITY AIRPLANE DATA

Point identification (a)	Condensing length, l_c, in.	Liquid mass flow rate, w_{liq}, lb/sec	Vapor mass flow rate, w_g, lb/sec	Inlet quality, x_o	Static pressure, psia							Temperature at condensing tube inlet, T_o, °F
					P_o	P_{12}	P_{24}	P_{36}	P_{48}	P_{60}	P_{72}	
1A	66	0.0416	0.0379	0.91	19.12	18.62	17.02	16.62	16.62	16.94	17.04	1080
1B	66	.042	.0379	.90	19.25	18.75	17.04	16.65	16.62	16.95	17.02	1080
1C	66	.042	.038	.90	18.93	18.42	16.75	16.40	16.35	16.70	16.80	1080
2A	66	.0424	.039	.92	19.47	18.95	17.35	17.05	17.07	17.43	17.76	1086
2B	66	.0422	.0351	.83	19.49	19.01	17.48	17.20	17.25	17.60	17.89	1086
3A	66	.042	.0378	.90	20.50	20.00	18.45	18.12	18.11	17.92	18.20	1095
4A	66	.0422	.0414	.98	20.33	19.83	18.15	16.80	17.88	18.10	18.40	1088
4B	66	.0424	.041	.97	20.50	19.97	18.35	18.25	18.15	18.30	18.71	1088
5A	66	.0434	.0399	.92	17.52	16.90	14.25	14.95	14.85	15.35	15.55	1086
5B	66	.0433	.0399	.92	18.54	18.04	17.13	17.02	15.90	16.28	16.69	1086
5C	66	.0433	.0394	.91	18.82	18.31	16.36	16.39	16.10	16.48	16.81	1086
6A	66	.0426	.04	.94	18.54	18.03	16.40	16.09	16.33	16.67	16.79	1107
7A	57	.0457	.0427	.94	17.67	17.17	15.58	15.43	15.60	15.94	16.08	1086
7B	57	.0415	.039	.94	18.18	17.65	16.00	15.86	16.03	16.34	16.50	1086
8A	66	.0416	.0395	.95	17.51	17.01	15.88	15.58	15.31	15.65	15.85	1086
8B	66	.0416	.0391	.94	18.80	18.29	16.55	16.25	16.46	16.84	16.95	1086
9A	66	.0428	.0399	.93	17.35	16.72	15.12	14.89	15.00	15.39	15.60	1086
10A	66	.0427	.0384	.90	18.38	17.88	16.08	16.18	15.73	16.13	16.33	1010
10B	66	.0427	.0384	.90	17.45	16.93	15.16	14.98	14.83	15.20	15.43	1010
11A	66	.0434	.0403	.93	17.33	16.70	15.50	13.50	14.00	15.20	15.38	1089
11B	66	.0417	.0390	.94	18.20	17.70	16.05	15.80	15.95	16.30	16.33	1089
12A	54	.0400	.0384	.96	17.98	17.30	15.88	15.80	16.20	16.42	16.70	1018
12B	54	.0398	.0382	.96	17.88	17.00	15.60	15.49	15.89	16.20	16.25	1018
12C	54	.0400	.0382	.96	17.88	17.05	15.65	15.55	15.96	16.30	16.40	1018
13A	52	.0410	.0384	.94	18.06	16.37	15.40	16.20	16.18	16.49	16.64	1056
13B	52	.0412	.0384	.94	17.38	16.76	15.38	15.22	15.70	15.90	16.02	1056
14A	63	.0422	.0392	.93	18.75	17.89	16.27	15.79	15.98	16.43	16.77	1056
14B	63	.0422	.0387	.92	18.60	17.70	16.00	15.53	15.64	16.02	16.42	1056
14C	63	.0428	.0382	.89	18.50	17.44	15.85	15.35	15.45	15.94	16.25	1056
15A	69	.0416	.0388	.93	18.85	18.69	17.14	16.26	16.15	16.34	16.63	1005
15B	69	.0418	.0387	.92	17.81	17.69	15.90	15.30	15.10	15.50	15.61	1005
15C	69	.0418	.0370	.89	18.24	18.15	16.40	15.76	15.56	15.94	16.03	1005
15D	69	.0418	.0373	.89	18.08	17.78	16.22	15.65	15.38	15.79	15.84	1005
16A	53	.0398	.0383	.96	18.75	18.22	16.83	16.70	16.95	17.44	17.58	1020
16B	53	.0397	.0391	.98	18.66	18.13	16.71	16.47	16.66	17.18	17.35	1020
16C	53	.0398	.0390	.98	18.43	17.93	16.53	16.34	16.63	17.03	17.21	1020
17A	54	.0395	.0395	1.00	18.75	18.23	16.83	16.61	16.86	17.30	17.63	1044
17B	54	.0396	.0396	1.00	18.41	17.91	16.53	16.28	16.51	16.93	17.16	1044
18A	54	.0396	.039	.98	18.66	18.14	16.78	16.60	17.00	17.21	17.42	1044
18B	54	.0396	.0380	.96	18.34	17.83	16.42	16.23	16.63	16.88	17.03	1044

[a]Number designates trajectory; A, early portion of trajectory; B, middle portion of trajectory; C, late portion of trajectory.

TABLE II. - Concluded. ZERO-GRAVITY AIRPLANE DATA

Point identification (a)	Condensing length, l_c, in.	Liquid mass flow rate, w_{liq}, lb/sec	Vapor mass flow rate, w_g, lb/sec	Inlet quality, x_o	Static pressure, psia							Temperature at condensing tube inlet, T_o, °F
					P_0	P_{12}	P_{24}	P_{36}	P_{48}	P_{60}	P_{72}	
19A	51	0.0405	0.0395	0.98	18.31	17.81	16.44	16.29	16.84	17.35	17.30	1050
19B	51	.0405	.039	.96	17.87	17.35	16.06	15.98	16.46	16.75	16.85	1050
19C	51	.0407	.0388	.95	17.71	17.20	16.00	15.38	16.36	16.70	16.75	1050
19D	51	.0405	.0387	.96	17.77	17.25	15.97	16.05	16.35	16.75	16.73	1050
20A	51	.0406	.0388	.95	18.03	17.53	16.31	16.21	16.65	16.91	17.08	1050
20B	51	.0407	.0388	.95	18.20	17.67	16.34	16.24	16.61	16.89	17.05	1050
21A	51	.0408	.0386	.98	18.28	17.78	16.45	16.26	16.71	17.38	17.22	1050
22A	57	.0413	.0386	.94	19.07	18.55	17.00	16.64	16.80	17.30	17.40	1050
23A	63	.0413	.0393	.95	18.25	17.75	-----	15.82	16.03	16.55	16.79	1000
23B	63	.0417	.0397	.95	18.16	17.65	-----	15.55	15.75	16.36	16.55	1000
24A	63	.0415	.0382	.92	18.00	17.47	-----	15.51	15.68	16.18	16.46	1000
24B	63	.0415	.0382	.92	17.70	17.20	-----	15.28	15.39	15.88	16.08	1000
25A	63	.0417	.0398	.96	18.42	17.90	-----	15.91	16.08	16.63	16.96	1000
25B	63	.042	.0392	.93	17.87	17.36	-----	15.24	15.33	15.87	16.26	1000
26A	57	.0425	.0381	.90	19.42	18.92	-----	17.30	17.64	18.00	18.01	1000
26B	57	.043	.0384	.89	19.77	19.26	-----	17.69	18.03	18.28	18.28	1000
27A	57	.0415	.0384	.97	20.78	19.77	-----	18.12	18.42	19.21	18.91	1000
27B	57	.0421	.0377	.90	19.86	19.38	-----	17.80	18.10	18.93	18.63	1000
28A	66	.0426	.0405	.95	20.52	19.48	-----	17.00	17.05	17.51	17.93	1000
28B	66	.0426	.0393	.92	20.00	19.00	-----	16.65	16.70	17.10	17.50	1000
29A	63	.0412	.0379	.92	16.86	15.44	-----	14.83	15.00	15.59	15.80	978
29B	63	.0412	.0382	.92	16.78	15.32	-----	14.80	14.90	15.50	15.70	978
30A	66	.0425	.0398	.94	17.62	16.03	-----	15.05	15.05	15.65	16.09	960
30B	66	.0426	.0409	.96	18.04	16.23	-----	15.30	15.17	15.79	16.28	960
30C	66	.0428	.0402	.94	18.01	16.32	-----	15.23	15.50	15.75	16.15	960
31A	54	.0426	.0385	.90	16.90	15.44	-----	15.47	15.88	15.59	16.48	946
32A	54	.0415	.0392	.94	18.33	16.41	-----	16.43	16.83	17.55	17.45	946
32B	54	.0418	.040	.96	18.41	16.98	-----	16.97	17.38	18.01	17.81	946
33A	48	.0392	.0388	.99	18.43	17.25	-----	17.85	18.33	18.50	18.45	963
33B	48	.0384	.0384	1.00	18.15	16.73	-----	16.88	17.69	17.95	17.85	963
34A	63	.0414	.0393	.95	19.52	18.14	-----	17.62	17.46	18.00	18.43	990
34B	63	.0415	.0393	.95	19.74	18.31	-----	17.63	17.71	18.13	18.43	990
35A	57	.0301	.0285	.95	17.98	17.24	-----	17.22	17.12	17.58	17.45	942
35B	57	.0303	.0273	.90	17.68	16.89	-----	16.67	16.77	17.35	17.11	942
36A	66	.0295	.0267	.90	18.37	17.65	-----	17.20	17.25	17.48	17.70	924
36B	66	.0290	.0282	.97	18.25	17.47	-----	17.00	17.05	17.28	17.45	924
37A	39	.0269	.0235	.87	15.63	15.38	-----	15.58	15.70	15.80	15.70	1000
37B	39	.027	.0233	.86	15.80	15.55	-----	15.75	15.85	15.95	15.84	1000
37C	39	.0273	.0227	.83	15.85	15.43	-----	15.62	15.73	15.83	15.68	1000
38A	41	.0275	.0236	.86	16.03	15.71	-----	15.87	16.16	16.30	16.10	1020
38B	41	.0279	.0236	.85	15.96	15.63	-----	15.83	16.13	16.23	16.02	1020
39A	45	.028	.0245	.88	15.90	15.43	-----	15.60	15.95	16.04	15.84	1100
39B	45	.028	.0241	.86	16.37	16.07	-----	16.19	16.50	16.58	16.31	1100
40A	48	.0279	.0244	.87	16.73	16.28	-----	16.38	16.78	16.88	16.71	1140
40B	48	.0280	.0239	.85	16.71	16.32	-----	16.38	16.81	16.86	16.66	1140
41A	51	.0278	.0243	.88	17.18	16.68	-----	16.58	16.88	17.08	16.98	1140
41B	51	.0280	.0246	.88	16.78	16.28	-----	16.18	16.48	16.68	16.48	1140

[a]Number designates trajectory; A, early portion of trajectory; B, middle portion of trajectory; C, late portion of trajectory.

TABLE III. - 1-g AND ZERO-GRAVITY AIRPLANE DATA

Gravity level, g's	Point identification (a)	Condensing length, l_c, in.	Liquid mass flow rate, w_{liq}, lb/sec	Vapor mass flow rate, w_g, lb/sec	Inlet quality, x_o	Static pressure, psia							Temperature at condensing tube inlet, T_o, °F
						P_0	P_{12}	P_{24}	P_{36}	P_{48}	P_{60}	P_{72}	
1	1	51	0.0288	0.0252	0.88	15.73	15.07	----	15.13	15.30	15.75	15.55	930
0	1A	51	.0270	.0267	.99	16.66	16.15	----	15.95	16.07	16.52	16.35	955
0	1B	51	.0274	.0263	.96	16.53	15.75	----	15.73	15.90	15.80	15.65	955
1	2	51	.0320	.0274	.86	16.97	16.20	----	16.23	16.47	16.89	16.73	1000
0	2A	52	.0292	.0290	.99	17.73	16.91	----	16.80	17.07	17.50	17.30	1000
0	2B	52	.0308	.0293	.95	17.80	16.81	----	16.79	17.08	17.41	17.21	1000
1	3	54	.0300	.0268	.90	17.70	16.88	----	16.81	17.00	17.24	17.30	1010
0	3A	54	.0290	.0280	.96	18.28	17.38	----	17.18	17.41	17.65	17.73	1010
0	3B	54	.0290	.0283	.98	18.17	17.27	----	17.09	17.30	17.50	17.63	1010
1	4	54	.0300	.0272	.91	18.03	17.20	----	17.03	17.31	17.70	17.55	1010
0	4A	55	.0288	.0278	.97	18.09	17.15	----	16.98	17.18	17.50	17.41	1010
1	5	57	.0300	.0269	.90	17.70	16.19	----	16.66	16.86	17.08	17.23	1040
0	5A	57	.0288	.0280	.97	18.57	17.73	----	17.45	17.73	17.90	18.03	1040
0	5B	57	.0290	.0277	.96	18.21	17.24	----	16.97	17.17	17.38	17.44	1040
1	6	57	.0300	.0270	.90	17.87	17.00	----	16.86	17.06	17.25	17.31	1030
0	6A	57	.0302	.0278	.92	18.13	17.32	----	17.01	17.22	17.40	17.48	1030
0	6B	57	.0290	.0262	.90	17.97	17.00	----	16.94	16.95	17.16	17.15	1030
1	7	63	.0300	.0280	.93	18.05	17.40	----	16.92	17.08	17.79	17.32	1040
0	7A	64	.0292	.0271	.93	18.41	17.53	----	17.06	17.31	17.46	17.61	1030
0	7B	64	.0292	.0269	.92	18.00	16.97	----	16.49	16.69	16.92	17.00	1030
1	8	63	.0300	.0280	.93	17.94	17.10	----	16.72	17.02	17.20	17.50	1030
0	8A	63	.0290	.0278	.96	18.30	17.32	----	17.01	17.23	17.39	16.98	1030
0	8B	63	.0290	.0270	.93	18.32	17.40	----	17.22	17.22	17.41	17.47	1030
1	9	66	.0300	.0286	.95	18.02	17.22	----	16.80	17.01	17.18	17.29	1030
0	9A	66	.0294	.0270	.92	18.79	17.90	----	17.43	17.64	17.74	17.94	1030
1	10	66	.0300	.0270	.90	17.94	17.12	----	16.70	16.90	17.07	17.16	1030
0	10A	66	.0300	.0268	.90	18.50	17.54	----	17.10	17.21	17.44	17.58	1030
1	11	39	.0300	.0257	.89	16.60	16.25	----	16.70	16.58	16.75	16.43	1000
0	11A	39	.0290	.0284	.98	16.85	16.39	----	16.93	17.05	17.30	16.55	1030
0	11B	39	.0290	.0282	.98	16.98	16.54	----	16.98	17.15	17.35	17.05	1030
1	12	42	.0302	.0266	.88	17.08	16.67	----	17.01	17.25	17.50	17.30	1130
0	12A	42	.0289	.0284	.98	18.25	17.62	----	17.40	18.20	18.40	18.11	1140
0	12B	42	.0291	.0279	.96	18.06	17.50	----	17.75	18.00	18.18	17.89	1130
1	13	42	.0300	.0269	.90	18.10	17.76	----	18.08	18.20	18.55	18.35	1040
0	13A	42	.0290	.0290	1.00	18.65	18.15	----	18.55	18.45	19.00	18.80	1050
0	13B	42	.0290	.0284	.98	18.30	17.70	----	18.15	18.35	18.57	18.32	1050
1	14	69	.0300	.0269	.90	19.25	18.70	----	18.12	18.08	18.35	18.30	1040
0	14A	69	.0290	.0290	1.00	20.10	19.50	----	18.92	18.90	19.10	19.15	1050
0	14B	69	.0294	.0294	1.00	19.70	19.06	----	18.48	18.46	18.67	18.68	1050
1	15	69	.0305	.0269	.88	19.35	18.75	----	18.20	18.20	18.44	18.43	1040
0	15A	69	.0291	.0291	1.00	20.11	19.47	----	18.86	18.76	19.05	19.06	1050
1	16	75	.0302	.0264	.88	19.34	18.73	----	18.06	18.04	18.26	18.41	1050
0	16A	75	.0292	.0286	.98	20.65	20.05	----	19.35	19.32	19.42	19.65	1050
1	17	75	.0298	.0267	.90	19.33	18.83	----	18.32	18.04	18.21	18.33	1050
0	17A	72	.0280	.0280	1.00	20.09	18.46	----	18.90	17.86	19.01	19.16	1050

[a] Number designates trajectory; A, early portion of trajectory; B, middle portion of trajectory; C, late portion of trajectory.

TABLE III. - Concluded. 1-g AND ZERO-GRAVITY AIRPLANE DATA

Gravity level, g's (a)	Point identification	Condensing length, l_c, in.	Liquid mass flow rate, w_{liq}, lb/sec	Vapor mass flow rate, w_g, lb/sec	Inlet quality, x_o	Static pressure, psia							Temperature at condensing tube inlet, T_o, °F
						P_o	P_{12}	P_{24}	P_{36}	P_{48}	P_{60}	P_{72}	
1	18	75	0.0391	0.0351	0.90	20.33	19.29	-----	18.26	18.08	18.37	18.69	1060
0	18A	82	.0387	.0387	1.00	22.18	21.15	-----	19.89	19.65	19.82	19.78	1070
0	18B	82	.0391	.0391	1.00	21.88	20.83	-----	19.79	19.65	19.83	19.79	1070
1	19	51	.0498	.0471	.94	17.88	15.75	-----	15.82	16.56	17.05	17.21	1000
0	19A	51	.0490	.0468	.95	18.49	16.23	-----	16.34	17.22	18.03	17.83	990
0	19B	51	.0491	.0480	.98	18.47	16.21	-----	16.28	17.09	17.93	17.73	990
1	20	75	.0500	.0473	.94	19.90	17.83	-----	16.85	16.70	17.30	17.23	1040
0	20A	75	.0480	.0465	.97	19.78	17.70	-----	16.70	16.70	17.30	17.23	1060
1	21	51	.0519	.0468	.90	18.05	15.92	-----	16.34	17.22	17.95	17.65	980
0	21A	60	.0518	.0534	1.00	20.85	18.07	-----	17.55	18.40	19.55	19.35	990
0	21B	60	.0516	.0523	1.00	20.10	17.23	-----	16.95	17.65	18.55	18.75	990
1	22	57	.0524	.0461	.88	19.08	17.10	-----	17.08	17.60	18.73	18.60	1090
0	22A	56	.0497	.0455	.91	18.61	16.50	-----	16.70	17.30	18.25	18.05	1080
1	23	66	.0507	.0460	.90	19.70	17.70	-----	17.04	17.24	17.88	18.30	1020
1	24	54	.0473	.0455	.96	18.33	16.60	-----	16.28	16.63	17.65	17.63	980
0	24A	54	.0431	.0436	1.00	18.64	16.72	-----	16.56	16.98	17.85	17.74	1000
1	25	51	.0482	.0437	.90	18.85	17.01	-----	16.97	17.58	18.33	18.25	1050
0	25A	52	.0472	.0459	.97	18.96	16.85	-----	16.76	17.35	18.28	18.13	1050
1	26	45	.0482	.0434	.90	18.38	16.40	-----	16.67	17.38	18.12	17.92	1100
0	26A	49	.0474	.0440	.93	17.91	15.16	-----	15.45	16.13	17.13	16.86	1100
0	27A	57	.0489	.0470	.96	19.67	17.48	-----	16.60	16.57	17.35	17.75	1100
1	28	75	.0496	.0446	.90	20.90	18.85	-----	17.50	17.15	17.60	17.65	1040
0	28A	75	.0485	.0456	.94	20.93	18.90	-----	17.60	17.30	17.71	17.83	1060
0	28B	75	.0483	.0457	.95	21.00	18.95	-----	17.61	17.30	17.75	17.85	1060
1	29	69	.0490	.0440	.90	21.00	19.03	-----	17.54	17.34	17.35	17.93	1190
0	29A	72	.0501	.050	1.00	20.95	18.75	-----	17.36	17.05	17.55	18.20	1090
0	29B	72	.0500	.0500	1.00	21.15	18.95	-----	17.48	17.17	17.65	18.23	1090
1	30	69	.0496	.0447	.90	20.50	18.42	-----	17.13	17.07	17.70	18.28	1060
0	30A	69	.0497	.0425	.85	19.45	17.38	-----	16.64	16.66	16.29	17.60	1070
1	31	66	.0503	.0435	.87	20.37	18.40	-----	17.37	17.62	18.20	18.60	1040
0	31A	66	.0493	.0400	.85	18.91	16.81	-----	16.23	16.35	17.20	17.26	1060
1	32	63	.0499	-----	----	18.07	16.13	-----	15.55	15.85	17.00	16.80	1040
0	32A	63	.0496	.0424	.86	18.72	16.75	-----	16.43	16.75	17.87	17.58	1060
0	32B	63	.0496	.0429	.86	18.88	16.92	-----	16.67	16.98	18.10	17.78	1060
1	33	57	.0501	.0423	.84	19.10	17.17	-----	16.85	17.35	18.45	18.15	1040
0	33A	57	.0494	.0427	.86	18.79	16.85	-----	16.67	17.07	18.10	18.82	1060
0	33B	57	.0494	.0435	.88	18.92	16.98	-----	16.75	17.17	18.18	17.90	1060
1	34	69	.0515	.0469	.91	20.30	18.27	-----	17.44	17.53	18.13	18.50	1040
0	34A	69	.0506	.0434	.86	18.70	16.70	-----	16.25	16.42	17.12	17.30	1040
1	35	63	.0500	.0467	.93	19.40	17.50	-----	16.80	17.15	18.40	18.30	1060
0	35A	63	.0490	.0464	.95	18.96	16.69	-----	16.25	16.58	17.83	17.58	1090
0	36A	56	.0492	-----	----	18.20	16.10	-----	16.32	16.92	17.80	17.65	1070
1	37	54	.0496	.0440	.89	19.92	18.90	-----	18.62	18.50	19.40	19.25	1050
0	37A	54	.0506	-----	----	18.73	16.59	-----	16.55	16.90	17.83	17.72	1070

[a] Number designates trajectory; A, early portion of trajectory; B, middle portion of trajectory; C, late portion of trajectory.

NASA-Langley, 1965 E-2580

"The aeronautical and space activities of the United States shall be conducted so as to contribute . . . to the expansion of human knowledge of phenomena in the atmosphere and space. The Administration shall provide for the widest practicable and appropriate dissemination of information concerning its activities and the results thereof."

—NATIONAL AERONAUTICS AND SPACE ACT OF 1958

NASA SCIENTIFIC AND TECHNICAL PUBLICATIONS

TECHNICAL REPORTS: Scientific and technical information considered important, complete, and a lasting contribution to existing knowledge.

TECHNICAL NOTES: Information less broad in scope but nevertheless of importance as a contribution to existing knowledge.

TECHNICAL MEMORANDUMS: Information receiving limited distribution because of preliminary data, security classification, or other reasons.

CONTRACTOR REPORTS: Technical information generated in connection with a NASA contract or grant and released under NASA auspices.

TECHNICAL TRANSLATIONS: Information published in a foreign language considered to merit NASA distribution in English.

TECHNICAL REPRINTS: Information derived from NASA activities and initially published in the form of journal articles.

SPECIAL PUBLICATIONS: Information derived from or of value to NASA activities but not necessarily reporting the results of individual NASA-programmed scientific efforts. Publications include conference proceedings, monographs, data compilations, handbooks, sourcebooks, and special bibliographies.

Details on the availability of these publications may be obtained from:

SCIENTIFIC AND TECHNICAL INFORMATION DIVISION

NATIONAL AERONAUTICS AND SPACE ADMINISTRATION

Washington, D.C. 20546